




Results of the Humanitarian Demining Sensors Field Test

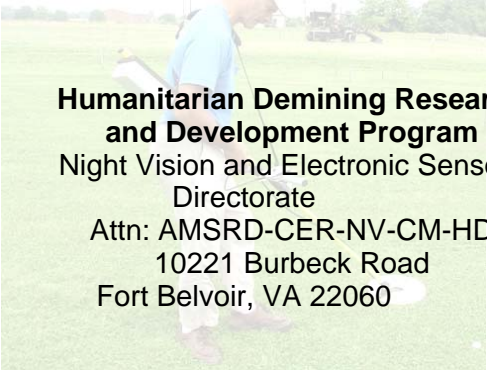
November 2002

Prepared by

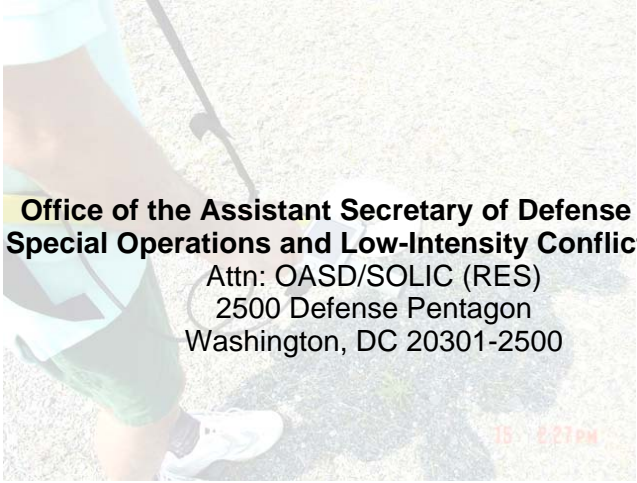


Institute for Defense Analyses
4850 Mark Center Drive
Alexandria, VA 22311-1882

for



**Humanitarian Demining Research
and Development Program**
Night Vision and Electronic Sensors
Directorate
Attn: AMSRD-CER-NV-CM-HD
10221 Burbeck Road
Fort Belvoir, VA 22060



**Office of the Assistant Secretary of Defense
Special Operations and Low-Intensity Conflict**
Attn: OASD/SOLIC (RES)
2500 Defense Pentagon
Washington, DC 20301-2500

Results of the Humanitarian Demining Sensors Field Test, November 2002

Elizabeth Ayers
Erik Rosen
Frank S. Rotondo
Jeremy Teichman

May 2005

INSTITUTE FOR DEFENSE ANALYSES
Science and Technology Division
4850 Mark Center Dr., Alexandria, VA 22311-1882

PREFACE

This document is an analysis of the results of a blind test of four landmine-detection systems developed by three contractors, Geo-Centers, Inc., Geophex, Ltd., and Stolar Horizon, Inc.. The blind test took place at a temperate U.S. test site during the period November 12-22 November 2002.

This document was prepared for the Director of Defense Research and Engineering, Office of the Under Secretary of Defense (Acquisition and Technology), under a task titled “Technical Support to Communications and Electronics Command Night Vision and Electronic Sensors Directorate Mine Detection Program.”

ONTENTS

EXECUTIVE SUMMARY	ES-1
I. INTRODUCTION	I-1
A. The Humanitarian Demining Program.....	I-1
B. System Descriptions.....	I-1
C. Test Procedures.....	I-2
D. Measures of Effectiveness	I-5
1. Position Accuracy and Bias	I-5
2. Detection Probability and False-Alarm Rate	I-6
3. Characterized Clutter	I-7
4. ROC Curves.....	I-8
5. Rate of Advance.....	I-8
6. Geophex Target Identification	I-8
7. Meteorological Data.....	I-8
II. TEST RESULTS.....	II-1
A. Position Accuracy and Bias	II-1
B. <i>FAR</i> and <i>P_d</i> Summaries.....	II-1
1. Geo-Centers	II-3
2. Geophex	II-4
3. Stolar EDIT-2.....	II-4
4. Stolar EDIT-3.....	II-6
C. Rate of Advance.....	II-7
III. CONCLUSIONS.....	III-1
Glossary	GL-1
APPENDIX A—Position Resolution Plots	A-1
APPENDIX B—ROC Curves.....	B-1
APPENDIX C—Geophex Target Identification Results	C-1
APPENDIX D—Meteorological Data.....	D-1

TABLES

ES-1.	Selected Test Results	ES-2
I-1.	Burial Depths of Mine and Clutter Targets.....	I-4
II-1.	Summary of the Monte Carlo Estimate of Fraction of Detections within R_{halo} for AP Mines with 4 cm Radii, Given Contractor Position Resolutions	II-2
II-2.	Geo-Centers FAR and P_d by Mine Category	II-3
II-3.	Geophex FAR and P_d by Mine Category	II-5
II-4.	Stolar EDIT-2 FAR and P_d by Mine Category.....	II-6
II-5.	Stolar EDIT-3 FAR and P_d by Mine Category.....	II-7
II-6.	Average Rate of Advance of the Systems.....	II-8

FIGURES

I-1.	(a) The Geo-Centers EFGPR; (b) the Geophex GEM-3; and (c) the Stolar EDIT System.....	I-3
I-2.	A Pictorial Definition of Detections and False Alarms	I-5
II-1.	Along-Track and Across-Track Biases and Standard Deviations Against AP Mines for the Different Contractor Systems.....	II-2
II-2.	Along-Track and Across-Track Biases and Standard Deviations Against AT Mines for the Different Contractor Systems.....	II-2

EXECUTIVE SUMMARY

INTRODUCTION

This document is an analysis of the results of a blind test of four landmine-detection systems developed by three contractors:

- Geo-Centers Energy-Focused Ground-Penetrating Radar (EFGPR);
- Geophex GEM-3 Mine Detector and Discriminator; and
- Stolar Electromagnetic-Wave Detection and Imaging Transceiver (EDIT-2 and EDIT-3).

The sensors were tested at a temperate U.S. test site in November 2002. The objective of the test was to establish the current performance of the systems against both antipersonnel (AP) and antitank (AT) mines in temperate environmental conditions.

TESTING

A set of on-road and off-road lanes 1.5 m wide by 25 m long was defined for the test. On-road lanes had a prepared gravel surface; off-road lanes were covered with clumpy grass. A variety of AT and AP mines were buried at tactical depths. The mines were either metal (M) or low metal (LM). Clutter, which consisted of spent shell casings and shrapnel from bounding fragmentation mines, was also added to the lanes.

Each system surveyed the lanes, and based on the data collected, we calculated detection probability (P_d), which is the fraction of mines detected, and the false-alarm rate (FAR) per square meter, which is the density of alarms not matched to a target. Other performance metrics were studied and are available in the body of this report.

RESULTS

Table ES-1 gives P_d s and FAR s for combined on-road and off-road testing.¹

¹ The FAR in this table includes naturally occurring and emplaced clutter; a further analysis of the FAR is provided in the body of the report.

Table ES-1. Selected Test Results

Category	Geo-Centers	Geophex	Stolar	
	EFGPR	GEM-3	EDIT-2	EDIT-3
FAR, m^{-2}	0.38	0.64	1.08	1.00
P_d				
AT-M	0.88	1.00	0.98	0.90
AP-M	0.48	0.98	0.67	0.64
AT-LM	0.84	0.47	0.92	0.86
AP-LM	0.46	0.85	0.57	0.46

CONCLUSIONS

The following conclusions can be drawn from this test:

- *Geo-Centers:* P_d and FAR performance was better on road than off road. AT mines were detected at higher rates than AP mines, regardless of depth and metal content.
- *Geophex:* The AT-LM mine category was the most challenging for detection. The road condition generally had little impact on P_d s, except for the AP-LM category, where the P_d was lower off road. The detector was generally very sensitive to objects of higher metal content. 63% of detected mines were identified correctly.
- *Stolar EDIT-2:* The detection rate for AT mines was higher than for AP mines. Within the AT and AP categories, the detection rates for metal mines were slightly higher than those for low-metal mines. Off road, AP detection was better than on road, but AT detection was worse. The FAR was not significantly affected by road condition.
- *Stolar EDIT-3:* The detection rate for AT mines was higher than for AP mines. Within the AT and AP categories, the detection rates for metal mines were slightly higher than those for low-metal mines. In most cases, the road condition did not affect P_d s significantly, except for the AP-M category where the P_d was higher off road. The FAR was not significantly affected by road condition.

I. INTRODUCTION

A. THE HUMANITARIAN DEMINING PROGRAM

The Humanitarian Demining Section of the U.S. Army Night Vision and Electronic Sensors Directorate (NVESD) is developing sensors to detect antitank (AT) and antipersonnel (AP) landmines. These sensors include the GEM-3 Mine Detector and Discriminator, built by Geophex, Ltd. of Raleigh, N.C.; the Energy-Focused Ground-Penetrating Radar (EFGPR), built by Geo-Centers Inc. of Newton, Mass.; and the hand-held Electromagnetic-Wave Detection and Imaging Transceiver (EDIT-2 and EDIT-3), built by Stolar Horizon, Inc., of Raton, N.M. These sensors were tested at a temperate U.S. test site in November 2002. The objective of the testing was to establish the current performance of the systems.

B. SYSTEM DESCRIPTIONS

Four systems were independently tested:

- *Geo-Centers Energy-Focused Ground-Penetrating Radar.* The Geo-Centers EFGPR is an array of synchronized-impulse radars. The impulse provides broadband radiation with a center frequency of approximately 1.25 GHz and a 3 dB bandwidth of about ± 850 MHz. The array consists of six transmit antennas and six receive antennas. The 12 antennas are forward mounted onto a cart that is motor driven. The width of the array is 1.25 m. A single operator is required to drive the cart. Sensor data is processed by an on-board computer, and automated target recognition (ATR) algorithms are used to make real-time mine declarations. Raw data is recorded so that playback using alternative detection algorithms is possible in post processing. In addition, the system can produce physical markings. A photo of the system is provided in Figure I-1(a).
- *Geophex GEM-3 Mine Detector and Discriminator.* The Geophex GEM-3 is a hand-held frequency-domain electromagnetic (EM) sensor operating in the band from about 270 Hz to 48 kHz. It consists of two transmit coils and a receive coil embedded in a circular plastic disk at the end of a telescopic wand having a maximum extension of about 2 m. Quadrature and in-phase EM spectra are recorded as the operator moves the sensor over the ground.

These spectra are compared to a library of target spectra to determine the presence of a mine. A photo of the system is provided in Fig. I-1(b).

- *Stolar Electromagnetic Wave Detection and Imaging Transceiver, EDIT-2 and EDIT-3.* The EDIT is a hand-held time-domain EM sensor and imaging system. The imaging capability was not used in this test. Instead, an audio signal indicated the presence of a mine. Two variants of EDIT, called the EDIT-2 and EDIT-3, were tested. The EDIT-2, an older design, was used extensively in prior field tests. The newer EDIT-3 system, a prototype, was designed to be more thermally stable and have a higher signal-to-noise (S/N) ratio than its predecessor. Stolar tested one EDIT-2 unit and two EDIT-3 units at this test, and these systems were assessed separately. A photo of the EDIT system (the two variants looked similar) is provided in Figure I-1(c).

C. TEST PROCEDURES

A set of lanes, each 1.5 m wide by 25 m long, was defined for the purpose of the testing. Lanes with prepared gravel surfaces and unprepared grassy surfaces served to replicate on-road and off-road conditions. A variety of AT and AP mines were buried in the lanes at tactical depths. All mines were classified according to their metal content. Generally, a mine is considered to be metal (M) if the mine's case (or other major structural element) is metal. For example, the VS50, a plastic-cased AP mine, would be placed in the AP-M category because it contains a relatively large metal reinforcing plate. Mines that are largely nonmetal, except for some metal parts in the fuzing or firing mechanism, are considered low-metal (LM) mines. For example, the M14 antipersonnel mine, whose metal content is less than 1 gram, would be placed in the AP-LM category. In addition to mine targets, characterized clutter was also buried in the test lanes. Clutter consisted of spent shell casings and shrapnel or "frag" from bounding fragmentation mines. Note that all mine and characterized clutter targets contained at least some metal. Table I-1 shows the burial depths of the various mine categories and clutter.

A complete survey of a lane by a detector system is referred to as a *mission*. Each detector system (one Geophex, one Geo-Centers, and two Stolar systems) completed four missions on a given lane, with two missions run in each direction.² Each system provided

² Lanes were surveyed in both directions to minimize the use of visual cues during testing and also to make position accuracy studies, which are discussed later, more meaningful.

(a)



(b)



(c)



Figure I-1. (a) The Geo-Centers EFGPR; (b) the Geophex GEM-3; and (c) the Stolar EDIT system

Table I-1. Burial Depths of Mine and Clutter Targets

Category	Distance from Surface to Top of Target (in.)
AT-M	5
AP-M	0.5
AT-LM	3
AP-LM	1
Clutter	0.5

a list of *declarations*, or locations of suspected mines, for each mission. The four systems also indicated a signal strength associated with each declaration. Finally, the time to complete each mission was noted. The systems differed in how missions were executed:

- Two operators from Geophex each completed two missions per lane, one run in each direction. The operators placed poker chips at the locations of suspected mines as the missions were in progress. Surveyors then measured the GPS coordinates of the declarations after the missions were completed.
- One operator from Stolar specialized in the EDIT-2 system, and another specialized in the usage of the EDIT-3. Each operator completed four missions per lane, and the results of the EDIT-2 and EDIT-3 were assessed separately. The operators placed poker chips at the locations of suspected mines as the missions were in progress. Surveyors then measured the GPS coordinates of the declarations after the missions were completed.
- Two operators from Geo-Centers shared the operation of the Geo-Centers cart system. Because the Geo-Centers system required two passes to cover the full width of the lane, one mission consisted of two passes that were then post-processed to form a single mission using a “stitching” algorithm run after the completion of the November testing. Because the system contained an integrated Global Positioning System (GPS), the post-processed declarations were provided in GPS coordinates.

Based on the data collected, the detection probability, false-alarm rate, position accuracy, and rate of forward progress of each system were computed. By raising the threshold on the confidence values, receiver-operator characteristic (ROC) curves were also generated. Each of these measures is defined in detail in the next section; Chapter II presents the results of the test.

D. MEASURES OF EFFECTIVENESS

1. Position Accuracy and Bias

We begin our analysis by compiling the distribution of *miss distances* in the along-track and across-track directions. The miss distance is defined as the difference between the position of a target and a declaration; the along-track and across-track directions are the directions in the 25 m length and 1.5 m width of the lanes, respectively. Miss-distance distributions generally derive their shape from two physical processes. First, a detector's response to clutter and noise contributes to a flat distribution—these declarations are distributed randomly in space with respect to a target because they are not associated with the detector's response to a target. Second, a detector's response to targets is peaked near target locations, generally displaying a Gaussian shape. The Gaussian describes the spatial response of the detector to the mines: the standard deviation of the Gaussian is related to the position accuracy of the detection process, and the mean of the Gaussian is related to the bias (or offset) of the detection process.³ This shape assumption (a Gaussian added to a flat distribution) is in fact an excellent match to the actual distributions.

To extract the position accuracy and bias of the detector, it is not adequate to compute the mean and standard deviation of the entire miss-distance distribution because random false alarms from clutter and noise contribute to these distributions. Ideally, we want only to measure the standard deviation and bias of the detector responding to a mine. We can separate these effects of detections and false alarms by fitting both the along-track and across-track distributions to the following function:

$$f(x) = c + a \cdot e^{-\frac{(x-m)^2}{2w^2}} . \quad (\text{I-1})$$

The constant term c represents the flat (random) distribution; the Gaussian parameters a , m , and w model the response of the detector system to the mines, with w and m representing the standard deviation and bias, respectively. The miss-distance data used in this analysis was binned in 5 cm bins, with the error in each bin taken to be the square root of the number of entries in the bin. If there were no entries in a bin, we took the error

³ This discussion assumes that the Gaussian's standard deviation and bias are due completely to the detector and ignores contributions such as survey errors. Since it is expected that the detector dominates these errors, this is probably a reasonable assumption.

to be 1. The fits were performed by finding the function parameters of f which minimize the χ^2 of the fit, where $\chi^2 = \sum_i (x_{\text{fit}} - x_i)^2 / \sigma_i^2$, and i is the index of a given bin.

Chapter II, Section A, gives the position accuracy and bias results, with detailed distributions given in Appendix A.

2. Detection Probability and False-Alarm Rate

Contractor declarations of potential target locations are either matched to an emplaced target, a “detection,” or not matched to a target, a “false alarm.” Declarations are matched to emplaced targets if the declaration is within a critical distance, R_{halo} , of the edge of the target. The value for R_{halo} is taken to be 15 cm. This distance criterion can result in more than one candidate declaration that matches a particular emplaced target. When there are redundant declarations within R_{halo} , the contractor is credited with a single detection of the target. Redundant detections are not counted as false alarms. If the declaration is within R_{halo} but outside the test lane, it is still scored as a valid detection. A declaration not within R_{halo} of any emplaced target and located within the test lane is considered a false alarm. These possible outcomes are illustrated in Figure I-2.

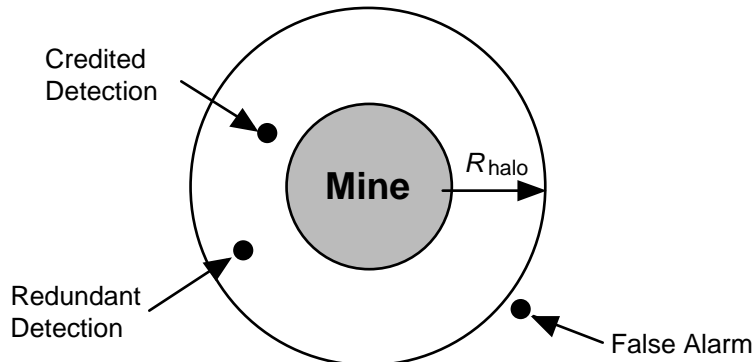


Figure I-2. A Pictorial Definition of Detections and False Alarms

The detection probability (P_d) and false-alarm rate (FAR) are the two primary measures derived from this type of blind test. The detection probability is simply the fraction of the encountered mines that are detected:

$$P_d = \frac{\# \text{ mines detected}}{\# \text{ mines encountered}} . \quad (\text{I-2})$$

This probability is computed for each mine category, as well as for each mine model. The false-alarm rate is the measure of the number of false alarms per square meter of operation for the detector:

$$FAR = \frac{\text{\# false alarms}}{\text{total lane area} - \text{area in halos}} . \quad (\text{I-3})$$

Ninety-percent confidence-level errors are computed on both the P_d and FAR . The 90-percent confidence-level errors on P_d are derived assuming a binomial distribution, using standard statistical procedures.⁴ The lower error is the value for P_d that would yield the measured P_d (or greater) with a 5-percent probability; the upper error is the value for P_d that would yield the measured P_d (or less) with a 5-percent probability. The error in FAR is derived by assuming that the collection of false alarms is a counting exercise; hence the standard deviation in the number of false alarms is given by the square root of the number of false alarms. The 90-percent confidence level errors are thus 1.65 times the standard deviation, a range that encompasses 90 percent of the statistical error in a normal distribution.

Chapter II, Section B, gives P_d and FAR results.

3. Characterized Clutter

In addition to natural, or background, clutter, the lanes contained characterized clutter that was emplaced as part of the design of the site. This characterized clutter requires additional analysis.

In general, the total FAR of a sensor is determined by properties of the natural environment as well as by the density of man-made clutter:

$$\text{total } FAR = \text{background } FAR + \rho_{cl}P_{fp} , \quad (\text{I-4})$$

where the background FAR is the false-alarm rate for that sensor against the natural environment of the site, ρ_{cl} is the man-made clutter density, and P_{fp} is the probability of false positive against man-made clutter (the probability that the emplaced clutter is called a mine).

We track the total FAR , the background FAR , and the P_{fp} for shells and fragments. Tracking the false positives against characterized clutter elucidates the discrimination capability of the sensor.

⁴ The computation for the confidence-level intervals on binomial distributions, performed by *MATLAB* in this analysis, is based on the discussion in N.L. Johnson, S. Kotz, and A.W. Kemp, *Univariate Discrete Distributions* (New York: John Wiley & Sons, 1993), pp. 124–130.

4. ROC Curves

For this test, contractors were asked not only to make target declarations, but to assign a confidence value to them. These confidence values⁵ were subjective for Stolar (on a scale from 1 to 5), miss-fit metrics for Geophex, and the output of a real-time ATR for Geo-Centers. For Stolar and Geo-Centers, the higher the confidence value, the greater the certainty that a mine is present. For Geophex, the smaller the miss-fit metric, the greater the certainty that a mine is present.

These alarm confidence values allow for the formation of ROC curves that relate P_D and FAR . These ROC curves can be more informative than the single-point performance measures computed in the absence of confidence values. The ROC curves give the cost in terms of the number of false alarms that it would take to detect a given percentage of mines. These curves can shed light on the ease or difficulty with which mines of a specific type are detected. ROC curves for each of the systems appear in Appendix B.

5. Rate of Advance

We measure the rate of advance of the operators by computing the number of seconds per square meter spent surveying the lanes. Chapter II, Section C, gives the results.

6. Geophex Target Identification

Geophex used a target-ID algorithm to compare the signals of the GEM-3 to a library of mine signatures. The degree to which the present signal matched each of the mine signatures stored in the library was quantified. The closest matched mine was identified, and a miss-fit parameter was computed. Data collectors recorded the miss-fit values and the mine names as called out by the Geophex operators. Results appear in Appendix C.

7. Meteorological Data

Meteorological data taken during the test period is provided in Appendix D.

⁵ Note that this confidence value, which is an indication of the operator's confidence in a declaration, should not be confused with the confidence-level errors discussed in Section I.D.2, which are measures of statistical accuracy.

II. TEST RESULTS

A. POSITION ACCURACY AND BIAS

As discussed in Chapter I, miss-distance distributions were constructed for each contractor against both AP and AT targets and fit to Eq. I-1. We grouped on-road and off-road data and data against metal and low-metal targets because there were no substantive differences in the distributions for these groups and the combined data provided better statistical samples for the fits. Figures II-1 and II-2 give the results for the fits for AP and AT mines, respectively. The detailed distributions, as well as the overall fits, can be seen in Appendix A.

As a first step to determine if the resolutions outlined in Figures II-1 and II-2 are adequate given the 15 cm R_{halo} , we compared the 3-standard-deviation widths derived from the figures with the sum of mine and halo radii, ($R_{\text{mine}} + R_{\text{halo}}$). In the case of AT mines, where typical radii are ~ 15 cm, the 3-standard-deviation distances are approximately equal to or less than the ($R_{\text{mine}} + R_{\text{halo}}$) distance. This means that very few declarations would fall outside the halo of an AT mine. For AP mines, whose radii are ~ 4 cm, some of the 3-standard-deviation distances are larger than the ($R_{\text{mine}} + R_{\text{halo}}$) distance. To determine if a halo radius of 15 cm is large enough to capture all detections, we ran a Monte Carlo simulation using the results of the bias and standard deviations of the miss-distance distributions for AP mines (see Table II-1). Note that the number of missed detections is small. If the position resolution of the device degrades, however, the resultant P_d may decrease substantially using an R_{halo} of 15 cm.

B. FAR AND P_d SUMMARIES

In this section we summarize the P_d vs. FAR results of each contractor. We pay particular attention to how the performance depends on road conditions, metal content of targets, depth of targets, and size of targets.

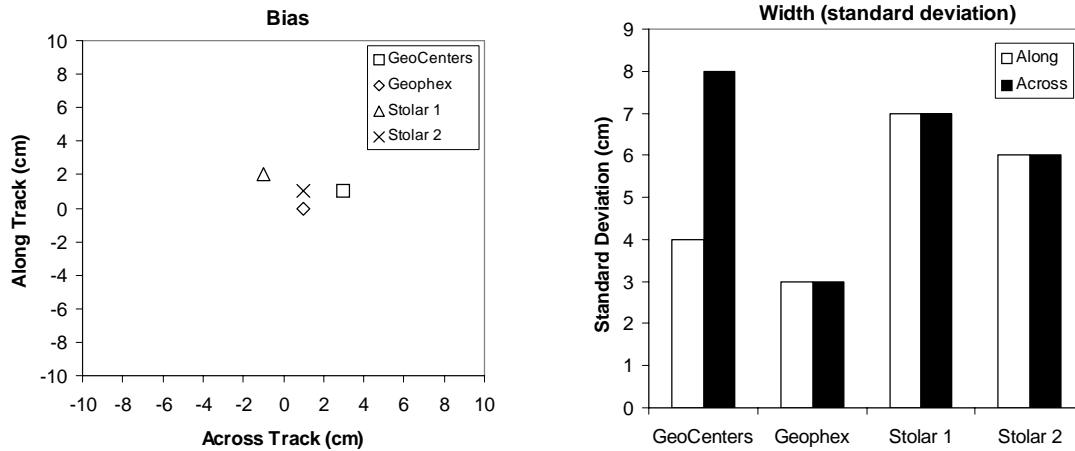


Figure II-1. Along-Track and Across-Track Biases and Standard Deviations Against AP Mines for the Different Contractor Systems

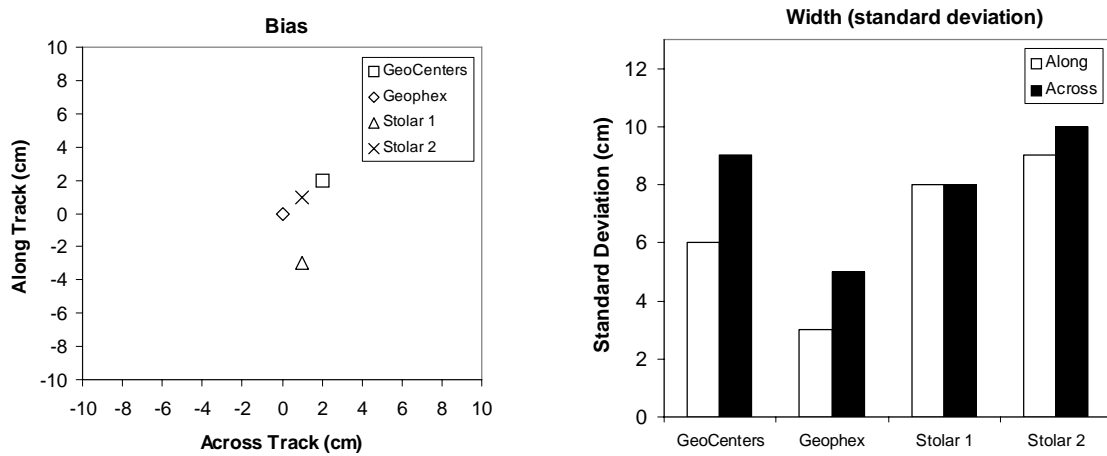


Figure II-2. Along-Track and Across-Track Biases and Standard Deviations Against AT Mines for the Different Contractor Systems

Table II-1. Summary of the Monte Carlo Estimate of Fraction of Detections within R_{halo} for AP Mines with 4 cm Radii, Given Contractor Position Resolutions

Contractor	Fraction of Detections within R_{halo} for APs
Geo-Centers	0.98
Geophex	1.00
Stolar 1	0.97
Stolar 2	0.99

1. Geo-Centers

Table II-2 gives the FAR , P_d , and P_{fp} summaries for Geo-Centers. These results are listed for the combined on-road and off-road conditions, as well as for on-road and off-road lanes separately. The Geo-Centers results exhibit the following properties:

- Geo-Centers' performance was strongly dependent on road surface—both FAR and P_d performance was better on road than off road.
- Geo-Centers' P_d was very dependent on mine size. Thus, AT mines were detected at higher rates than AP mines, in spite of their greater burial depths and regardless of metal content. In particular, we note that AT-LM mines were detected at a higher rate than AP-M mines.
- Within the AT or AP categories, Geo-Centers' P_d was only slightly better for metal mines than for low-metal mines.

Table II-2. Geo-Centers FAR and P_d by Mine Category (90% Confidence-Level Limits)

		$FAR (m^{-2})$	
		avg.	90% CL range
GeoCenters	total	0.38	0.41 - 0.36
	bkgnd	0.37	0.39 - 0.35
On & Off Road		P_d	
		avg.	90% CL range
AT-M		0.88	0.95 - 0.75
AP-M		0.48	0.59 - 0.38
AT-LM		0.84	0.90 - 0.77
AP-LM		0.46	0.54 - 0.38
		P_{fp}	
		avg.	90% CL range
Clutter 1		0.09	0.13 - 0.06
Clutter 2		0.05	0.09 - 0.03
Clutter 3		0.08	0.12 - 0.05

GeoCenters		$FAR (m^{-2})$	
		avg.	90% CL range
total		0.30	0.33 - 0.27
bkgnd		0.27	0.30 - 0.24
On Road		P_d	
		avg.	90% CL range
AT-M		1.00	1.00 - 0.86
AP-M		0.75	0.87 - 0.59
AT-LM		0.95	0.99 - 0.87
AP-LM		0.68	0.78 - 0.57
		P_{fp}	
		avg.	90% CL range
Clutter 1		0.13	0.20 - 0.07
Clutter 2		0.11	0.19 - 0.06
Clutter 3		0.13	0.20 - 0.07

GeoCenters		$FAR (m^{-2})$	
		avg.	90% CL range
total		0.45	0.48 - 0.42
bkgnd		0.45	0.49 - 0.42
Off Road		P_d	
		avg.	90% CL range
AT-M		0.75	0.90 - 0.54
AP-M		0.22	0.37 - 0.11
AT-LM		0.70	0.82 - 0.57
AP-LM		0.19	0.30 - 0.11
		P_{fp}	
		avg.	90% CL range
Clutter 1		0.05	0.11 - 0.02
Clutter 2		0.00	0.03 - 0.00
Clutter 3		0.03	0.08 - 0.01

- Overall, the false-positive rates on characterized clutter were quite low and slightly higher on road than off road. The addition of this clutter added only slightly to the *FAR* (compare total and background *FARs*).
- It is possible that a good fraction of the background *FAR* was due to bulk road properties as opposed to discrete metallic clutter, given the system's relative insensitivity to the characterized clutter at the site.

2. Geophex

Table II-3 gives the *FAR*, P_d , and P_{fp} summaries for Geophex. These results are listed for the combined on-road and off-road conditions, as well as for on-road and off-road lanes separately. The Geophex sensor exhibited the following properties:

- By far the most difficult mine target for the Geophex sensor was the AT-LM category. Recall that these mines are low-metal, like the AP-LM category but buried more deeply.
- The background *FAR* was significantly higher off road compared with on road.
- The road condition had little impact on the mine P_d s, except for AP-LM, which was lower off road than on road.
- The road condition had little impact on the P_{fp} s, except in the case of clutter type 2, which was detected more easily on road than off road.
- Overall, the detector was more sensitive to mines and characterized clutter with larger metal content, as well as to those buried less deeply.

3. Stolar EDIT-2

Table II-4 gives the *FAR*, P_d , and P_{fp} summaries for Stolar EDIT-2. These results are listed for the combined on-road and off-road conditions, as well as for on-road and off-road lanes separately. The Stolar EDIT-2 sensor exhibited the following properties:

- The detection rate for the AT mines was higher than that for the AP mines both on road and off road. This difference was most pronounced in the on-road lanes.
- Detection rates were slightly higher for metal mines than for low-metal mines within the AT and AP categories.
- Off road, AP detection was better (in particular AP-M) than on road, but AT detection was worse.
- The road surface did not have an appreciable effect on the *FAR*.
- The P_{fp} was low overall and especially low off road.

Table II-3. Geophex FAR and P_d by Mine Category (90% Confidence-Level Limits)

		FAR (m^{-2})	
		avg.	90% CL range
Geophex	total	0.64	0.68 - 0.61
	bkgnd	0.40	0.43 - 0.38

		P_d	
		avg.	90% CL range
On & Off Road	AT-M	1.00	1.00 - 0.93
	AP-M	0.98	1.00 - 0.93
	AT-LM	0.47	0.56 - 0.38
	AP-LM	0.85	0.90 - 0.78

		P_{fp}	
		avg.	90% CL range
Clutter 1		0.99	1.00 - 0.97
Clutter 2		0.59	0.65 - 0.53
Clutter 3		0.97	0.99 - 0.94

		FAR (m^{-2})	
		avg.	90% CL range
Geophex	total	0.39	0.43 - 0.36
	bkgnd	0.12	0.14 - 0.10

On Road

		P_d	
		avg.	90% CL range
AT-M		1.00	1.00 - 0.86
AP-M		1.00	1.00 - 0.91
AT-LM		0.46	0.58 - 0.35
AP-LM		0.92	1.00 - 0.82

		P_{fp}	
		avg.	90% CL range
Clutter 1		1.00	1.00 - 0.97
Clutter 2		0.67	0.75 - 0.58
Clutter 3		0.99	1.00 - 0.95

		FAR (m^{-2})	
		avg.	90% CL range
Geophex	total	0.86	0.91 - 0.81
	bkgnd	0.64	0.68 - 0.60

Off Road

		P_d	
		avg.	90% CL range
AT-M		1.00	1.00 - 0.86
AP-M		0.97	1.00 - 0.86
AT-LM		0.48	0.61 - 0.35
AP-LM		0.77	0.86 - 0.65

		P_{fp}	
		avg.	90% CL range
Clutter 1		0.99	1.00 - 0.95
Clutter 2		0.52	0.61 - 0.43
Clutter 3		0.95	0.98 - 0.89

Table II-4. Stolar EDIT-2 FAR and P_d by Mine Category (90% Confidence-Level Limits)

		FAR (m^{-2})	
		avg.	90% CL range
Stolar EDIT-2	total	1.08	1.12 - 1.04
	bkgnd	1.04	1.08 - 1.00

On & Off Road

		P_d	
		avg.	90% CL range
AT-M	0.98	1.00 - 0.89	
AP-M	0.67	0.77 - 0.56	
AT-LM	0.92	0.96 - 0.86	
AP-LM	0.57	0.65 - 0.49	

		P_{fp}	
		avg.	90% CL range
Clutter 1	0.27	0.33 - 0.22	
Clutter 2	0.15	0.20 - 0.11	
Clutter 3	0.18	0.23 - 0.13	

		FAR (m^{-2})	
		avg.	90% CL range
Stolar EDIT-2	total	1.11	1.17 - 1.05
	bkgnd	1.05	1.11 - 1.00

On Road

		P_d	
		avg.	90% CL range
AT-M	1.00	1.00 - 0.86	
AP-M	0.59	0.74 - 0.43	
AT-LM	0.95	0.99 - 0.87	
AP-LM	0.53	0.64 - 0.42	

		P_{fp}	
		avg.	90% CL range
Clutter 1	0.35	0.44 - 0.27	
Clutter 2	0.22	0.30 - 0.15	
Clutter 3	0.24	0.33 - 0.17	

		FAR (m^{-2})	
		avg.	90% CL range
Stolar EDIT-2	total	1.05	1.10 - 1.00
	bkgnd	1.04	1.09 - 0.98

Off Road

		P_d	
		avg.	90% CL range
AT-M	0.95	1.00 - 0.78	
AP-M	0.75	0.87 - 0.59	
AT-LM	0.89	0.95 - 0.78	
AP-LM	0.62	0.73 - 0.49	

		P_{fp}	
		avg.	90% CL range
Clutter 1	0.20	0.28 - 0.13	
Clutter 2	0.08	0.15 - 0.04	
Clutter 3	0.13	0.19 - 0.07	

4. Stolar EDIT-3

Table II-5 gives the FAR , P_d , and P_{fp} summaries for Stolar EDIT-3. These results are listed for the combined on-road and off-road conditions, as well as for on-road and off-road lanes separately. The Stolar EDIT-3 sensor exhibited the following properties:

- The detection rate for AT mines was higher than that for the AP mines both on road and off road. This difference was most pronounced on road.
- Detection rates were slightly higher for metal mines than for low-metal mines within the AT and AP categories. This effect was largest for AP mines off road.

Table II-5. Stolar EDIT-3 FAR and P_d by Mine Category (90% Confidence-Level Limits)

		FAR (m^{-2})	
		avg.	90% CL range
Stolar EDIT-3	total	1.00	1.03 - 0.96
	bkgnd	0.97	1.00 - 0.93

		P_d	
		avg.	90% CL range
On & Off Road	AT-M	0.90	0.97 - 0.79
	AP-M	0.64	0.74 - 0.53
	AT-LM	0.86	0.91 - 0.79
	AP-LM	0.46	0.54 - 0.38

		P_{fp}	
		avg.	90% CL range
On & Off Road	Clutter 1	0.26	0.31 - 0.20
	Clutter 2	0.14	0.18 - 0.10
	Clutter 3	0.17	0.22 - 0.12

		FAR (m^{-2})	
		avg.	90% CL range
Stolar EDIT-3	total	0.99	1.04 - 0.93
	bkgnd	0.94	1.00 - 0.89

		P_d	
		avg.	90% CL range
On Road	AT-M	0.90	0.98 - 0.72
	AP-M	0.53	0.68 - 0.37
	AT-LM	0.84	0.91 - 0.74
	AP-LM	0.43	0.55 - 0.32

		P_{fp}	
		avg.	90% CL range
On Road	Clutter 1	0.32	0.41 - 0.24
	Clutter 2	0.16	0.24 - 0.10
	Clutter 3	0.19	0.28 - 0.13

		FAR (m^{-2})	
		avg.	90% CL range
Stolar EDIT-3	total	1.01	1.06 - 0.95
	bkgnd	0.99	1.04 - 0.94

		P_d	
		avg.	90% CL range
Off Road	AT-M	0.90	0.98 - 0.72
	AP-M	0.75	0.87 - 0.59
	AT-LM	0.89	0.95 - 0.78
	AP-LM	0.48	0.60 - 0.36

		P_{fp}	
		avg.	90% CL range
Off Road	Clutter 1	0.20	0.28 - 0.13
	Clutter 2	0.11	0.18 - 0.07
	Clutter 3	0.15	0.22 - 0.09

- Road condition did not seem to affect detection rates except for the AP-M category, which had a higher detection rate off road.
- The road surface did not have an appreciable effect on the FAR.
- The P_{fp} was low overall and lower off road than on road.

D. RATE OF ADVANCE

We measured the rate of advance of the operators by computing the number of seconds per square meter spent surveying the lanes. Table II-6 gives the results. The Geo-Centers result includes the multiple passes that the system made on each lane.

Recall that, for a given lane excursion, Geo-Centers scanned the lane with its system aligned on the left side of lane, drove the system back to the beginning of the lane, and then scanned the lane again in the same direction but with the array aligned with the right side of the lane. Those two scan times were summed to arrive at the total time it took for one lane excursion.

Table II-6. Average Rate of Advance of the Systems

System	Avg. Advance Rate sec/m²
Geo-Centers	6.3
Geophex	123
Stolar EDIT-2	51
Stolar EDIT-3	55

III. CONCLUSIONS

The following conclusions can be drawn from the humanitarian demining tests that took place in November 2002:

- *Geo-Centers*: P_d and FAR performance was better on road than off road. AT mines were detected at higher rates than AP mines, regardless of depth and metal content. False-positive rates on characterized clutter were generally low and added only slightly to the total FAR .
- *Geophex*: The AT-LM mine category was the most challenging for detection. The road condition generally had little impact on mine P_{ds} , except for the AP-LM category, where the P_d was lower off road. The P_{fp} s were high and contributed significantly to the total FAR . The detector was generally more sensitive to mines and characterized clutter with greater metal content. 63% of detected mines were identified correctly.
- *Stolar EDIT-2*: The detection rate for AT mines was higher than for AP mines. Within the AT and AP categories, the detection rates for metal mines were slightly higher than those for low-metal mines. Off road, AP detection was better than on road, but AT detection was worse. The total FAR was not significantly affected by road condition, and contributions from false positives were low.
- *Stolar EDIT-3*: The detection rate for AT mines was higher than for AP mines. Within the AT and AP categories, the detection rates for metal mines were slightly higher than those for low-metal mines. In most cases, the road condition did not affect P_{ds} significantly except for the AP-M category where the P_d was higher off road. The total FAR was not significantly affected by road condition, and contributions from false positives were low.

GLOSSARY

ρ_{cl}	man-made clutter density
AP	antipersonnel
AT	antitank
ATR	automated target recognition
CV	confidence value
EDIT	electromagnetic-wave detection and imaging transceiver
EFGPR	energy-focused ground-penetrating radar
EM	electromagnetic wave
<i>FAR</i>	false-alarm rate
GPS	Global Positioning System
LM	low metal
M	metal
NVESD	Night Vision and Electronic Sensors Directorate
P_d	detection probability
P_{fp}	probability of false positive
ROC	receiver-operator characteristic
S/N	signal to noise

APPENDIX A

POSITION RESOLUTION PLOTS

The data points in Figures A-1 through A-4 are the measured along-track and across-track miss-distance distributions for AP and AT mines as obtained by Geo-Centers, Geophex, and the two Stolar systems, respectively. When Eq. I-1 is fit to these distributions as shown by the solid curves in the figures, biases and resolutions can be extracted. These are listed in each figure. Because no substantive differences appear in any of the on-road/off-road or metal/low-metal distributions, these cases are grouped in the plots.

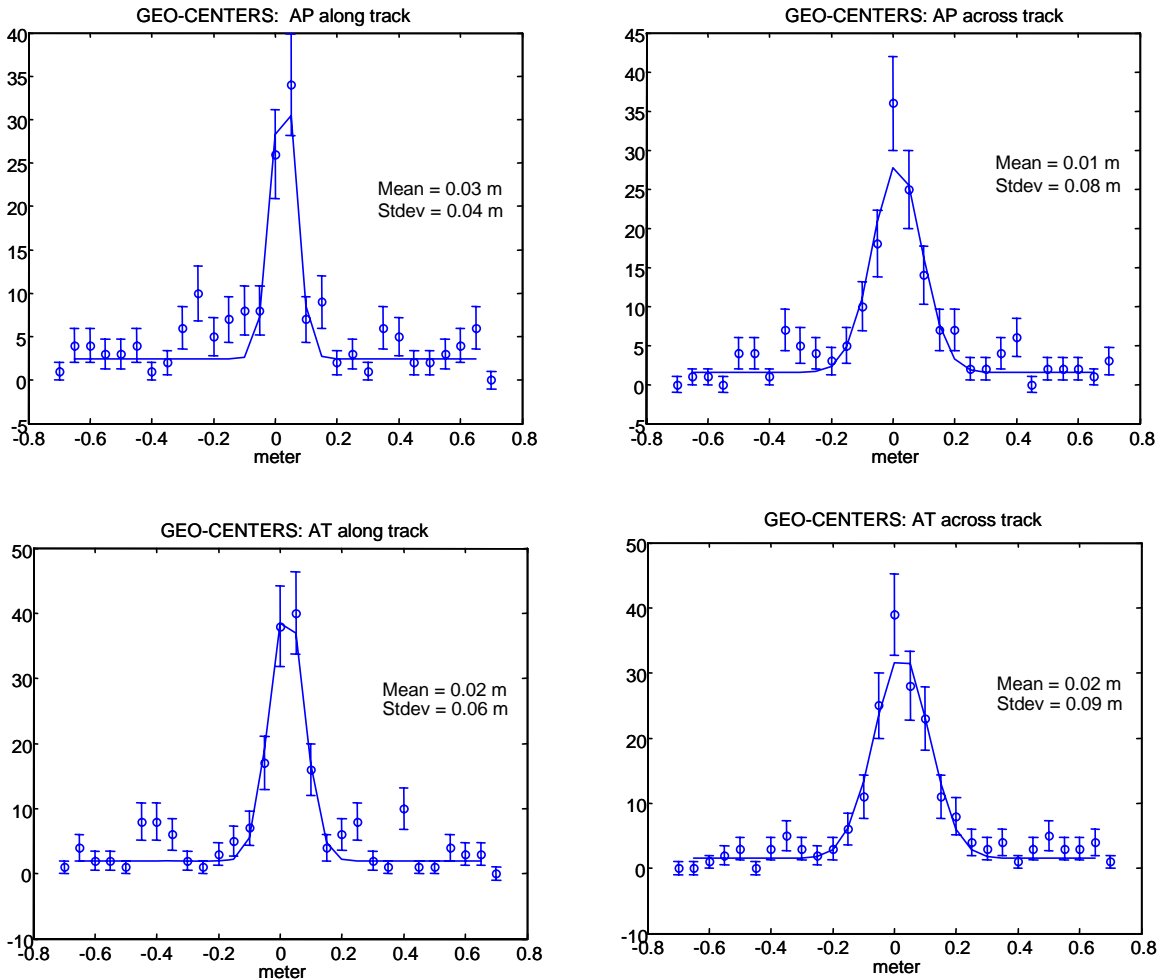


Figure A-1. Along-Track and Across-Track Miss Distance Distributions for AP Mines (top) and AT Mines (bottom) for the Geo-Centers System

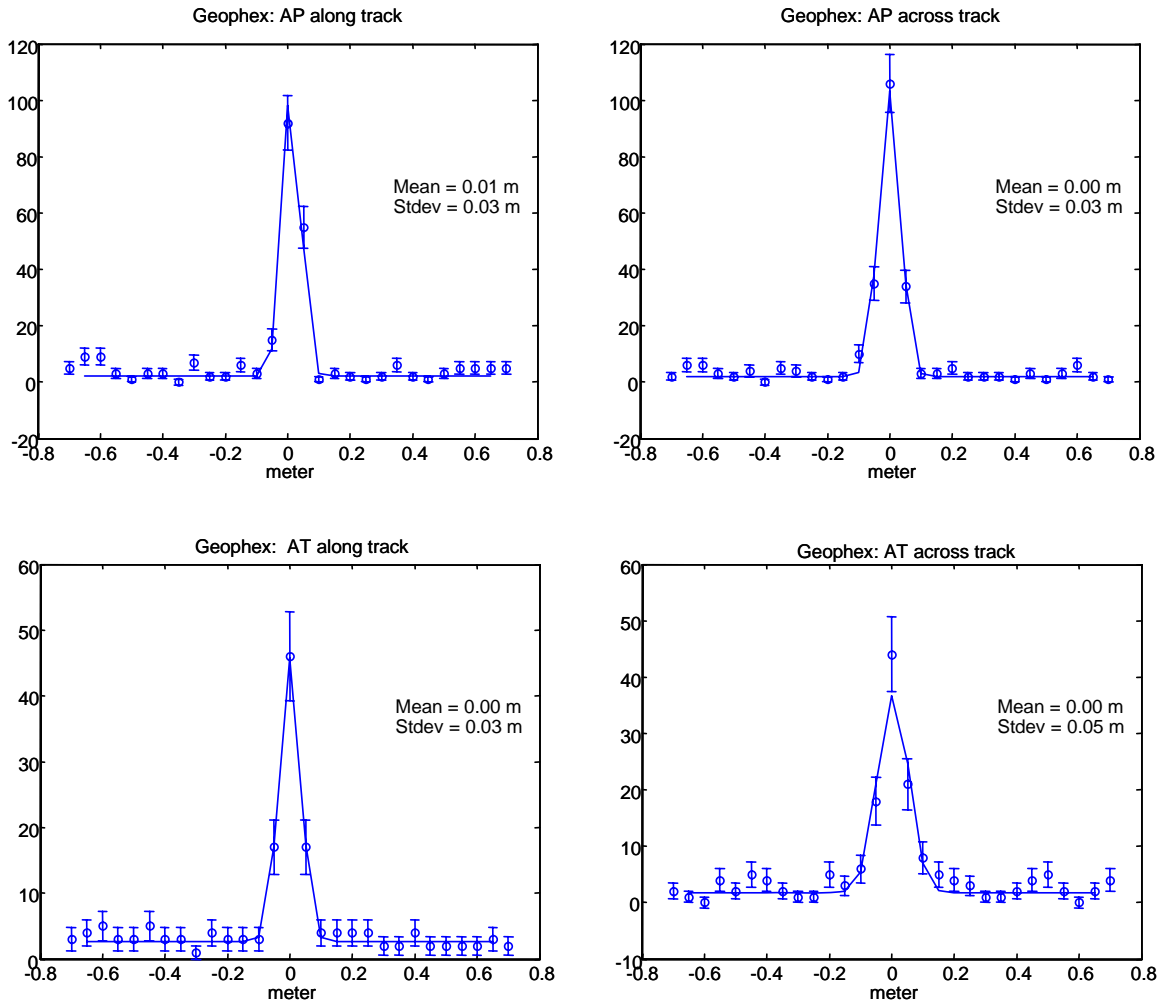


Figure A-2. Along-Track and Across-Track Miss Distance Distributions for AP Mines (top) and AT mines (bottom) for the Geophex system

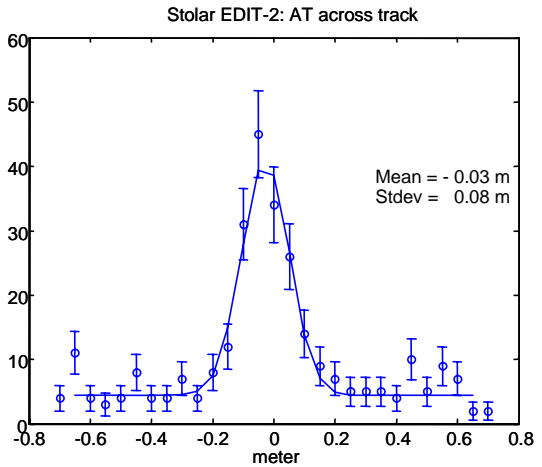
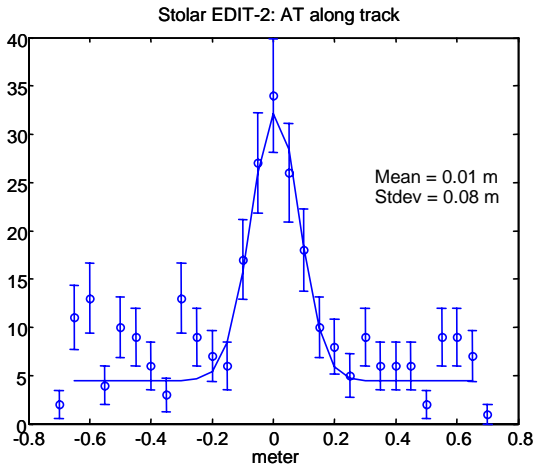
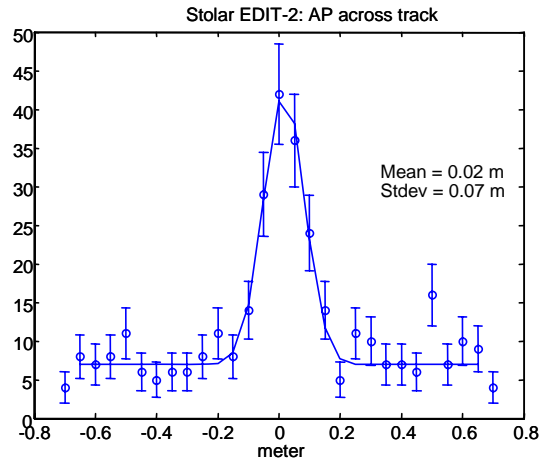
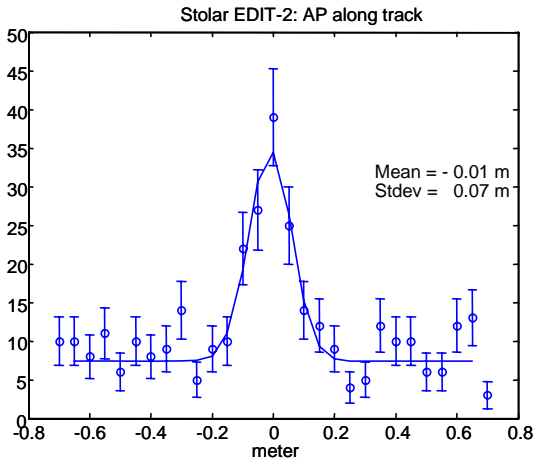


Figure A-3. Along-Track and Across-Track Miss Distance Distributions for AP Mines (top) and AT mines (bottom) for the Stolar EDIT-2 System

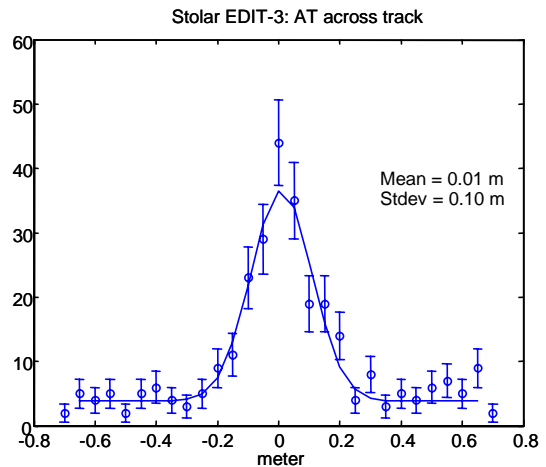
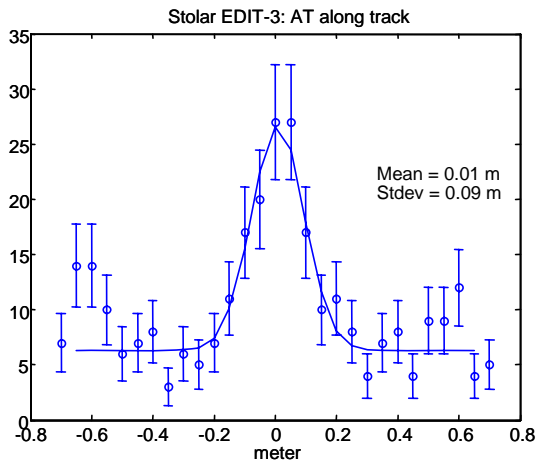
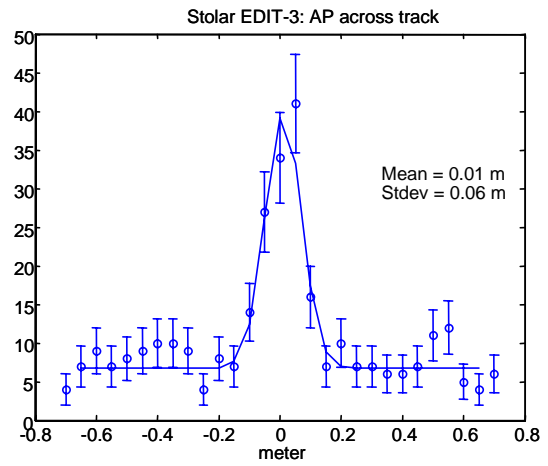
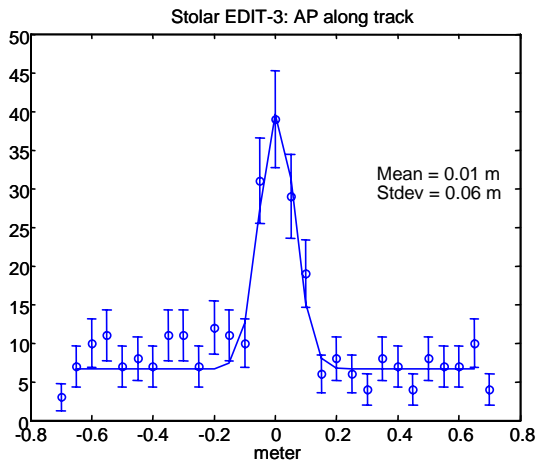


Figure A-4. Along-Track and Across-Track Miss Distance Distributions for AP Mines (top) and AT mines (bottom) for the Stolar EDIT-3 System

APPENDIX B

ROC CURVES

In this appendix, we show the receiver-operator characteristic (ROC) curves for each of the systems. For each system, ROC curves are given for the four mine categories—AT-M, AT-LM, AP-M, and AP-LM (see Chapter II). Results are for on and off road combined. The far right points from each of the curves correspond to the P_d s and FAR s in the tables from Chapter II.

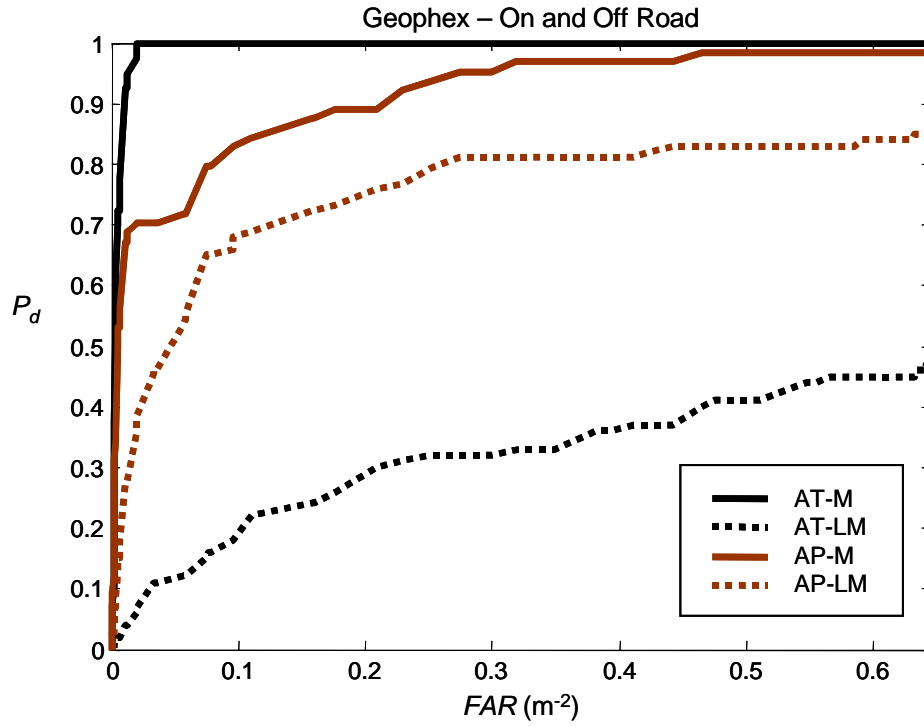


Figure B-1. ROC Curves for the Geo-Centers System for On and Off Roads Combined

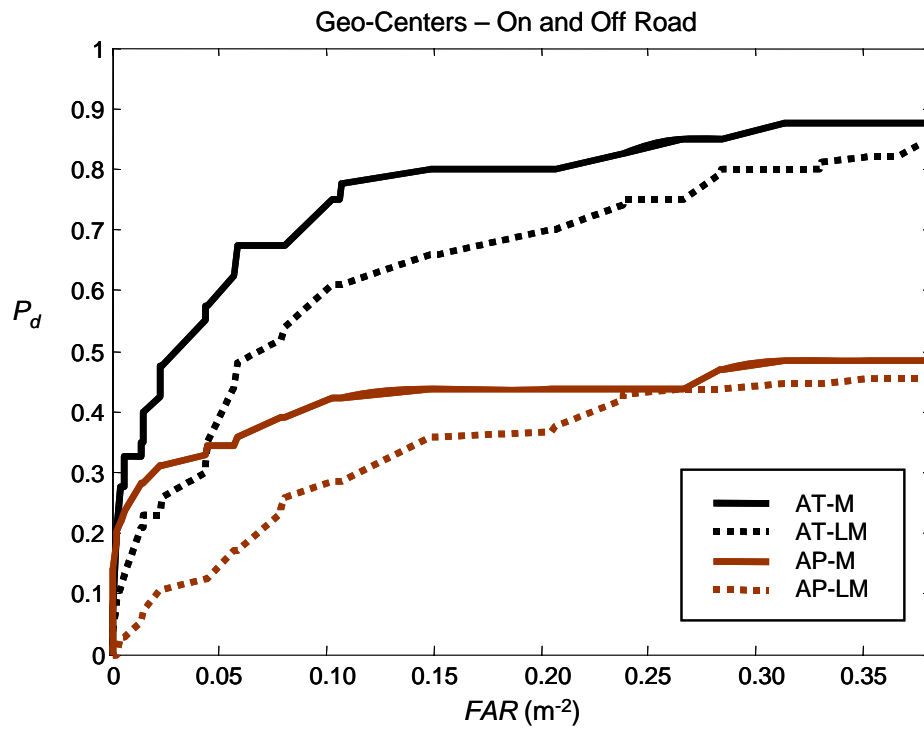


Figure B-2. ROC Curves for the Geophex System for On and Off Roads Combined

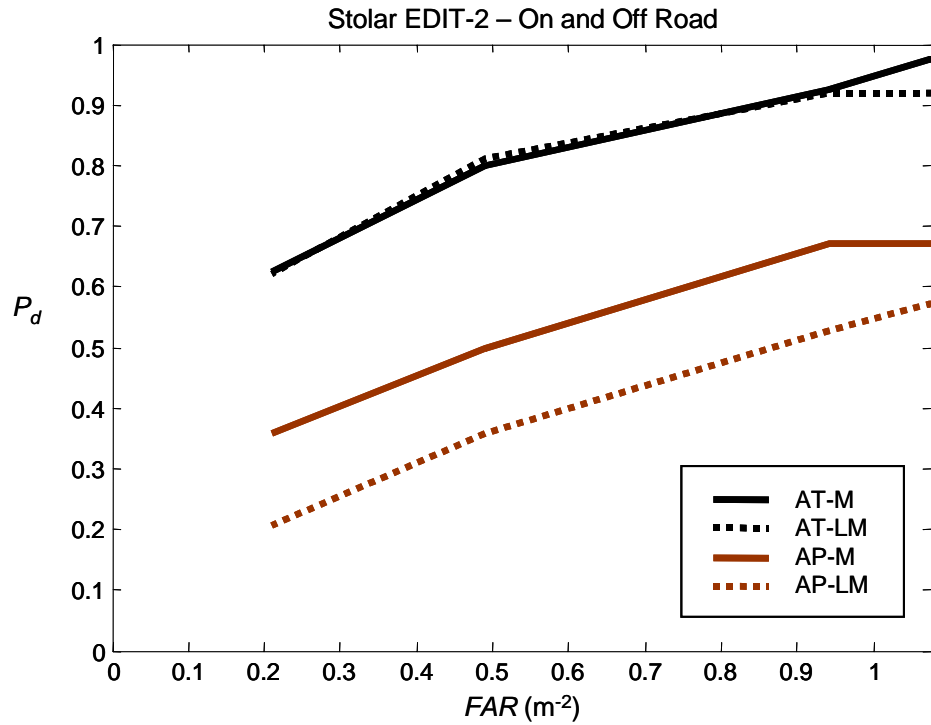


Figure B-3. ROC Curves for the Stolar EDIT-2 System for On and Off Roads Combined

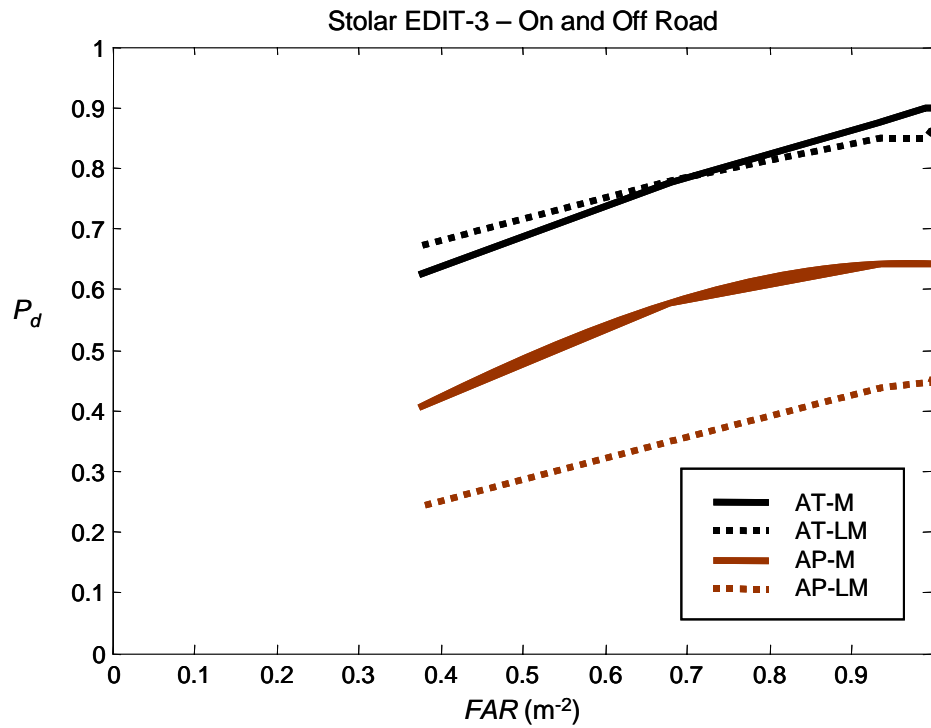


Figure B-4. ROC Curves for the Stolar EDIT-3 System for On and Off Roads Combined

APPENDIX C

GEOPHEX TARGET IDENTIFICATION RESULTS

Geophex used a target-ID algorithm to compare the signals of the GEM-3 with a library of mine signatures. The degree to which the present signal matched each of the mine signatures stored in the library was quantified. The closest matched mine was identified, and a miss-fit parameter was computed. Data collectors recorded the miss-fit values and the mine names as called out by the Geophex operators.

Table C-1 shows the accuracy of their mine identifications. The left-most column lists the mine and clutter types buried on the lanes that Geophex scanned. The top row of the table lists the various mine types that were declared by Geophex. The table includes data from detections only.

The following general conclusions are made with reference to Table C-1:

- 63% of detected mines were identified correctly;
- When detected, the mine types 7, 8, and 13 were identified correctly 100 percent of the time;
- Mine types 5, 9, and 14 were almost always misidentified;
- Emplaced clutter was almost never identified as clutter; instead, it was typically misidentified as mine types 1 and 12.

Table C-1. Results of Geophex Target Identifications

Truth	Type	Declared																		Total	
		Mine 1	Mine 2	Mine 3	Mine 4	Mine 5	Mine 6	Mine 7	Mine 8	Mine 9	Mine 10	Mine 11	Mine 12	SIM	SIM1	SIM12	SIM20	SIM3	SIM9		Clutter
Mine 1	AP-LM	27	1									1		3	3			2			37
Mine 2	AT-LM										1			1							2
Mine 3	AT-M			16	6					2											24
Mine 4	AP-M			2	13																15
Mine 5	AP-LM	10	1			1		1						2		1					16
Mine 6	AT-M			2			8			6											16
Mine 7	AT-LM							19													19
Mine 8	AP-LM									31											31
Mine 9	AP-LM	8												3							11
Mine 10	AP-M			1						15											16
Mine 11	AT-LM		1								2			1			1			1	6
Mine 12	AT-LM	1	1			1					2	6		6		2				1	20
Mine 13	AP-M												16								16
Mine 14	AP-M								1				15								16
Clutter 2	CL-M	21	5			10			2		20	7	1	35	7			1			109
Clutter 3	CL-M	71				1		1				1	102	1						1	178
Clutter 1	CL-M	21						3	7				133	13						6	183
	Total	159	9	21	19	13	8	24	41	23	25	15	267	65	10	3	1	3	0	9	

APPENDIX D

METEOROLOGICAL DATA

Figure D-1 shows the air temperature, precipitation, and soil moisture data collected during the test period. Measurements between the hours of 8 a.m. and 5 p.m. are displayed for a given day on each plot, with small gaps inserted between the days. The soil moisture data came from probes buried 1 in. below the soil surface.

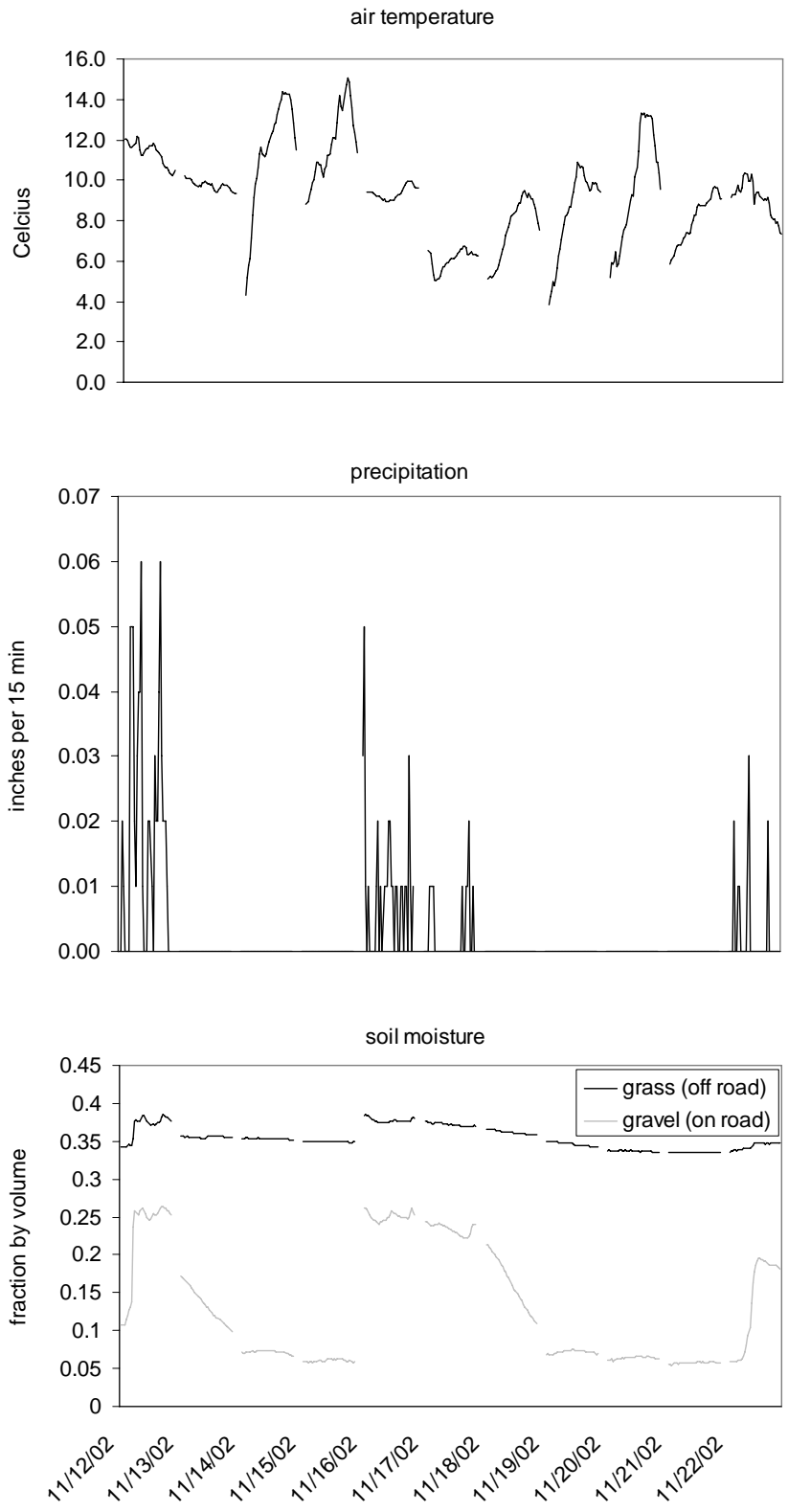


Figure D-1. Meteorological Data Taken During the Test